Journal of Electronic Materials (32) 6, 2003.

Predicting Tensile Properties of the Bulk 96.5Sn-3.5Ag Lead-free Solder*

Yi-Wen Cheng and Thomas A. Siewert
National Institute of Standards and Technology
Boulder, Colorado 80305-3328

Equations are presented for predicting tensile properties as functions of temperature and strain rate for the bulk eutectic 96.5Sn-3.5Ag lead-free solder. At 25 °C, we obtained 49.0 GPa for Young's modulus based on acoustic measurements, which is higher than most of those measured by tensile tests that are subject to viscoelastic creep; 23.1 MPa and 26.3 MPa for yield stress and UTS of specimens that are cast, annealed, and aged at a strain rate of 2.0×10^{-4} s^{-1}; 48.7 % for total elongation, which is larger than most of the reported values. The presence of "initial defects" in the specimens, such as porosity and void, might cause the reduction in measured total elongations.

Keywords: lead-free solders; stress-strain curve; tensile properties; tin-silver eutectic

---

Introduction

The tin-silver eutectic, which has a chemical composition of 96.5 percent tin and 3.5 percent silver (96.5Sn-3.5Ag) by mass, is one of the candidate lead-free alloys for replacing lead-containing solders, which are subject to concern over their effects on the health and environment. Although the tin-silver eutectic has been used as a solder in the past, published data on its tensile properties from different sources vary considerably. Many factors contribute to the differences in the reported properties, including different testing techniques and procedures, different specimen geometries, and different processing and treatment of specimens, which produce different microstructures.

Tensile properties are fundamental benchmarks for a solder and are used for comparison of materials, development of new materials, and quality control. In addition, the properties are the essential input parameters for structural design, and numerical modeling and simulation of mechanical behavior of materials in structures or devices. For solders used in the electronic industry, the temperature and strain rate experienced by a device during service vary widely, from –55 °C to 160 °C and from 10^{-1} to 10^{-6} s^{-1}. Temperature and strain rate are known to affect the tensile properties of solders significantly. It is desirable to express the properties as functions of temperature and strain rate so they can be easily incorporated into modeling and simulation analyses.

We have collected and analyzed available data on tensile properties of the bulk 96.5Sn-3.5Ag solder. Based on the analysis of the available data, we have derived equations for (1) Young's modulus as a function of temperature, and (2) 0.2 % offset yield stress and ultimate tensile strength as functions of temperature and strain rate for specimens that have been cast, annealed at about 150 °C, and aged at room temperature. Total elongation is expressed as a

function of the strain-rate sensitivity, which is the exponent in the relationship between flow stress and strain rate. From the yield stress and ultimate tensile strength, we also present a scheme to estimate the stress-strain curve for the solder under conditions where it does not exhibit continuous work-hardening and drastic softening during tensile testing.

Young's Modulus

Young's modulus is an important design parameter, which determines the amount of elastic deformation that a structure will exhibit under loading. It is one of the most structure-insensitive mechanical properties and is affected only slightly by alloying additions, heat treatment, or cold work[1]. For example, the value of Young's modulus for austenitic stainless steels, which contain chromium and nickel contents of approximately 20 % and 10 % by mass respectively, is different by less than 7 % from that of a typical carbon steel[1].

However, as shown in figure 1, reported values of Young's modulus for the 96.5Sn-3.5Ag solder vary widely. A value as low as 2.35 GPa (not shown in figure 1) at room temperature has been reported[10]. This is because the temperature range at which the solder is tested is usually higher than half of its homologous temperature. At this temperature range, viscoelastic and viscoplastic deformations, which depend on deformation rate, become important and significant. Caution must be taken if Young's modulus is to be determined from stress-strain curves obtained from tensile tests. To obtain an accurate value, testing must be performed at low stresses so that minimal yielding occurs and at a strain rate high enough to eliminate viscoplastic effects. It was reported[11] that a testing ramp speed equivalent to 80 MPa/s was sufficient to minimize the viscoplastic effects in the 60Sn-40Pb solder at 25 °C. The ramp speed of 80 MPa/s is equivalent to a strain rate of 2.07×10^{-3} s^{-1} for the solder.

Acoustic techniques, which use low stresses and high strain rates, are preferable methods for the determination of Young's modulus for solders. From the elastic constants of tin and silver obtained by acoustic methods[12-14], we calculated Young's moduli as a function of temperature. Then, we estimate Young's modulus of the 96.5Sn-3.5Ag solder using the linear rule of mixtures. The results given in figure 1 are different by less than 4 % from those reported by Vianco et al.[8], who used an acoustic method for the entire temperature range. It appears that values obtained with acoustic methods are consistent with limited scatter over a wide range of temperatures. Table 1 lists values of Young's modulus for the solder from various sources. Results obtained from tensile tests, except those of McCabe and Fine[6], show consistently low values[7,10,15]. To obtain the Young's modulus, McCabe and Fine used different strain rates in the experiments and some extrapolations in the analysis to exclude the time-dependent contributions.

Yield Stress

Yield stress is typically taken to be the stress at a specified small value of plastic strain, usually 0.2 % offset. Yield stress of a given alloy is affected by composition, microstructure, prior loading history, loading rate, and temperature. The dependence of yield stress on strain rate of the 96.5Sn-3.5Ag solder is, however, relatively weak, as reported by Tomlinson and Fullylove[16] with a strain-rate sensitivity of less than 0.1.

Published data of yield stress for the 96.5Sn-3.5Ag solder are limited. Based on the results of Harada and Satoh[10], Madeni et al.[17], Mavoori and Chin[18], and NCMS[7], we develop the following equation to describe the yield stress as functions of temperature and strain rate:

$$\sigma_y = -23.66 + 45.85\left(\frac{298}{T+273}\right)\left(\frac{\dot{\varepsilon}}{0.0001}\right)^{0.0285}, \qquad (1)$$

where σ_y is the 0.2 % offset yield stress in MPa, T is the test temperature in °C, and $\dot{\varepsilon}$ is the strain rate in s^{-1}. The data available for the development of the above equation are from –50 °C to

150 °C in temperature and from 1.0×10^{-5} s^{-1} to 1.0×10^{-2} s^{-1} in strain rate. The specimens used by Harada and Satoh were machined from cast ingots and then aged at room temperature for 240 h before testing. Others were also machined from cast ingots, but annealed at 150 °C for 16 to 24 h, followed by aging for a few days at room temperature.

Unlike Young's modulus, the yield stress is strongly influenced by microstructure. At room temperature (25 °C) and a strain rate of 8.33×10^{-4} s^{-1}, eq (1) predicts a value of 25.0 MPa, which is about half of the value reported by Hwang and Vargas[19], who tested specimens that were machined from cold-rolled strips. Higher strengths are expected from a cold-rolled than from a cast microstructure. Because of the microstructure-dependent nature of the property, eq (1) is applicable only to the solder that is cast, annealed, and aged.

Ultimate Tensile Strength

The ultimate tensile strength (UTS) of a given alloy is the maximum load obtained from a tensile test divided by the original cross-sectional area of the specimen. For alloys that are tested at temperatures higher than half of the homologous temperature, the true stress-true strain curve often exhibits a stress plateau, a steady-state condition, shortly after yielding. This behavior will be further discussed later in this paper.

If such a steady-state behavior is observed, the UTS of the alloy can be estimated from creep data, which are more commonly available for solders than UTS data. The power-law creep equation of the 96.5Sn-3.5Ag solder is given by Mavoori et al.[20] as

$$\dot{\varepsilon} = A\sigma^n \exp\left(\frac{-Q}{RT}\right), \qquad (2)$$

where $\dot{\varepsilon}$ is strain rate in s^{-1}, σ is the applied stress in MPa, R = 8.314 J/(mol·K) is the universal gas constant, T is temperature in K, $A = 1.5 \times 10^{-6}$, n = 11.3, and Q = 79500 J/mol. Rearranging eq (2), we obtain

$$\sigma = [\frac{\dot{\varepsilon}}{A}\exp(\frac{Q}{RT})]^{\frac{1}{n}}. \quad (3)$$

σ, computed from eq (3) as a function of temperature and strain rate, is taken to approximate the UTS of the solder for cast, annealed, and aged specimens. At room temperature (25 °C) and a strain rate of 2.0×10^{-4} s^{-1}, eq (3) predicts a UTS of 26.3 MPa, compared to 27 and 27.6 MPa as reported by NCMS[7] and Madeni et al.[17], respectively. The predicted value is within 4 % of the measurements made at different laboratories with specimens having similar casting, annealing, and aging treatments.

Similar to yield stress, UTS is strongly affected by microstructure. For the cold-rolled specimens, Hwang and Vargas[19] reported a value of 57.6 MPa, which is twice the value predicted for annealed specimens. For cast specimens that received no annealing treatment, Thwaites and Hampshire[21] reported values more than 50 % higher than our prediction for strain rates of 3.3×10^{-5} and 3.3×10^{-2} s^{-1}, Xiao et al.[22] reported values slightly higher than our predictions at three temperatures and three strain rates, while Satoh[15] reported a value of 20 MPa at the strain rate of 1.5×10^{-4} s^{-1}. The differences in UTS reported by these investigators can be attributed to the difference in cooling rates during casting when they prepared their specimens. Equation (3) is applicable only to the solder that is cast, annealed, and aged due to microstructure-dependent nature of UTS.

Elongation

Elongation determined from a uniaxial tensile test is an important material property, and the total elongation e_f is defined as

$$e_f = \frac{L_f - L_0}{L_0}, \quad (4)$$

where L_0 and L_f are gage lengths of the specimen before test and after fracture, respectively. Although elongation is not directly used in component design, it does serve as an indicator for the strain tolerance of a material and is often used in material specifications.

The measured e_f after a tension test depends on the gage length over which the measurement is taken. This is because an appreciable fraction of the plastic deformation concentrates in the necked region of the specimen. If the gage length is short, the contribution to the overall elongation from the necked region will be relatively large. Therefore, the gage length along with e_f should be given. It is also useful to report the uniform elongation, which is measured excluding the necked region. For an equivalent measure of e_f from specimens of different sizes, the ratio of L_0/D_0 for round bars or $L_0/\sqrt{A_0}$ for sheets has to be the same[1], where D_0 and A_0 are respectively the initial diameter and the initial cross-sectional area of the specimen.

It is common to observe wide scatter in the reported values for a given material from different sources because e_f of a specimen is specimen geometry-dependent and not all the tests reported in the literature use the same standardized specimen. However, elongation does reflect the ability of a material to deform plastically and has been shown to correlate well with the strain-rate sensitivity of the material[23]. In fact, the total percent elongation $\%e_f$ has been modeled[24] as a function of the strain-rate sensitivity m for non-strain-hardening materials, as

$$\%e_f = [(\frac{1}{f})^m - 1] \cdot 100, \tag{5}$$

where f is the index for "initial defect size" in tensile specimens. A least-squares regression of the data given by Woodford[23] gives a value of 0.011 for f.

From tensile tests with different strain rates, m is determined from

$$\sigma = C\dot{\varepsilon}^m, \tag{6}$$

where σ is the stress at a given strain and a given temperature, C is a constant, and $\dot{\varepsilon}$ is the strain rate. For a given material, m may vary slightly with temperature, strain, and strain-rate range. It is suggested that m be computed from a large strain in the stress-strain curve. The value of m is also equal to the reciprocal of the stress exponent n in eq (2). Using 0.011 for f and 0.088 (reciprocal of n in eq (3), which is 11.3) for m, we obtain 48.7 for $\%e_f$, which is about twice the value reported by NCMS[7] and Madeni et al.[17] for the cast and annealed specimens at room temperature. To match their $\%e_f$ values, f needs to be adjusted to 0.09, which implies that the "initial defect size" is larger for their specimens. This is consistent with the observation that specimens with lower elongations typically have porosities or voids[17]. $\%e_f$ values of 40, 34, and 31 were also reported[15,21].

Because many factors influence $\%e_f$, especially the specimen geometry, which is not considered in the equation, use of eq (5) with a fixed value of f provides only a guide to estimate the values of $\%e_f$. Well designed experiments are needed to quantitatively determine the value of f and the effect of specimen geometry.

Stress-strain curves

One of the stress-strain curves of the 96.5Sn-3.5Ag solder from Madeni et al.[17] is reproduced in figure 2. Their tests were conducted under displacement control with a constant displacement rate. The original curve is plotted in the coordinate of engineering stress and engineering strain, which are computed with the initial cross-sectional area and the initial gage length of the specimen. As shown in the figure, the stress increases initially, reaches a peak at a strain less than 0.05, and then decreases gradually with increasing strain. Madeni et al. assumed that necking (reduction in area) of the round-bar tensile specimens started right after the maximum engineering stress was reached.

For some materials under certain testing conditions, discernible necking in round-bar tensile specimens does not take place immediately after the maximum engineering stress is reached[24,25]. It is possible that the behavior of the solder shown in figure 2 falls into this category. If we re-plot figure 2 using true stress and true strain as shown in figure 3, the observed softening behavior in figure 2 disappears except at the very end of the engineering stress-versus-engineering strain curve. True stress σ and true strain ε, which take into account the continuous changes in gage length and cross-sectional area during test, better represent the true deformation characteristics, and are related to engineering stress s and engineering strain e by

$$\sigma = s(e+1), \tag{7}$$

$$\varepsilon = \ln(e+1). \tag{8}$$

Equations (7) and (8) apply only if, during test, constancy of volume and uniform deformation along the gage length are assumed.

Stress in figure 3 starts from the 0.2 % offset yielding. As shown in the figure, the stress increases initially as the solder hardens after yielding and then reaches a steady-state condition. The steady state is caused by dynamic recovery counterbalancing the effect of strain hardening. The commonly used power-law equation

$$\sigma = K\varepsilon^n \tag{9}$$

cannot adequately describe this type of stress-strain curve, which is frequently observed in steels tested at temperatures above half of their homologous temperatures[26]. Instead, the following equation has been used to fit the curves[26]:

$$\sigma = \sigma_y + (\sigma_{ss} - \sigma_y)[1 - \exp(-\beta\varepsilon)]^n. \tag{10}$$

Here, σ_y is obtained from eq (1), σ_{ss} is the steady-state stress and is estimated with a value 10 % higher than that computed from eq (3), β is a constant related to the hardening behavior, and n is

a constant related to the relationship between applied stress and dislocation density. n is set at a value of 0.65. β is treated as a function of temperature (in °C) and strain rate (in s^{-1}), and is estimated from

$$\beta = 56\left(\frac{T+273}{298}\right)^{2.3}\left(\frac{\dot{\varepsilon}}{0.0001}\right)^{-0.125}. \qquad (11)$$

Figure 4 shows a comparison between a predicted curve using eq (10) and those of Madeni et al.[17] for specimens tested at 25 °C and a strain rate of 2.0×10^{-4} s^{-1}.

The scheme presented here to estimate the stress-strain curves is applicable to those materials that exhibit steady-state behavior. For certain microstructures combined with some testing conditions, the solder might show continuous hardening or soften drastically because of microstructural changes due to dynamic recrystallization. Under these circumstances, the present scheme will not work well.

Summary

Equations have been developed for predicting tensile properties as functions of temperature and strain rate for the bulk 96.5Sn-3.5Ag lead-free solder. The properties include Young's modulus, 0.2 % offset yield stress, ultimate tensile strength, and total elongation. Young's modulus is little affected by microstructure and small compositional variations; because of time-dependent viscoelastic and viscoplastic contributions to displacements in the tensile tests, values measured from tensile tests are usually lower compared with values obtained using acoustic methods. Although well-designed tensile tests and analysis can give results that agree well with those obtained with acoustic techniques, the latter methods are better suited for the determination of Young's modulus of the solder, especially for a wide range of temperatures.

Yield stress and ultimate tensile strength are affected not only by temperature and strain rate, but also by processing that influences microstructure. The equations developed in this study

are based on data obtained with specimens that were cast, annealed, and aged before testing. Not enough information on microstructure associated with reported strength properties warrants the effort to quantitatively correlate properties to microstructure. What is needed are systematic experiments that measure the properties of specimens that are well controlled in processing and well characterized in microstructure. From such results, it may be possible to correlate the properties with microstructure or processing.

The major factors affecting total elongation are the strain-rate sensitivity of a material that does not exhibit continuous work-hardening, and the “initial defect size”, such as the presence of porosity and voids in the specimens. Specimen geometry also influences the value of the total elongation. This study also presents a scheme to estimate the stress-strain curves of the solder as functions of temperature and strain rate.

References

1. G. E. Dieter, Mechanical metallurgy, second edition, New York: McGraw-Hill (1976).

2. M. H. Biglari, M. Oddy, M. A. Oud, and P. Davis, Proc. Int. Symp. Electron. Goes Green 2000+, Berlin, Germany (September 11-13, 2000), p. 73.

3. R. Darveaux, K. Banerji, A. Mawer, and G. Doby, in: Ball Grid Array Technology, ed. John H. Lau, New York: McGraw-Hill (1995), p. 379.

4. H. Ledbetter and S. Kim, unpublished results, National Institute of Standards and Technology, Boulder, CO.

5. J. H. Lau and Y. H. Pao (editors), Solder Joint Reliability of BGA, CSP, Flip Chip, and Fine Pitch SMT Assemblies, New York: McGraw-Hill (1997).

6. R. J. McCabe and M. E. Fine, Scr. Mater. 39 189 (1998).

7. National Center for Manufacturing Sciences (NCMS), Technical Reports for the Lead Free Solder Project: Properties Reports: "Room Temperature Tensile Properties for Lead Free Solders"; Lead Free Solder Project CD-ROM, National Center for Manufacturing Sciences (1999).

8. P. Vianco, D. Frear, F. Yost, and J. Roberts, Development of alternatives to Pb-based solders, Sandia Report SAND97-0315, Sandia National Laboratories, Albuquerque, NM (1997).

9. P. T. Vianco, J. A. Rejent, A. F. Fossum, and M. K. Neilsen, in: Proc. 4th Pacific Rim Int. Conf. Adv. Mater. and Process., ed. S. Hanada et al., The Japan Institute of Metals (2001), p. 2925.

10. M. Harada and R. Satoh, in: Proc. 40th ECTC, Las Vegas, NV (May 20-23, 1990), p. 510.

11. J. W. Kilinski, J. R. Lesniak, and B. I. Sandor, in: Solder Joint Reliability: Theory and Applications, ed. John H. Lau, New York : van Nostrand Reinhold (1991), p. 384.

12. D. G. House and E. V. Vernon, Brit. J. Appl. Phys. 11 254 (1960).

13. J. R. Neighbours and G. A. Alers, Phys. Rev. 111 707 (1958).

14. Y. A. Chang and L. Himmel, J. Appl. Phys. 37 3567 (1966).

15. R. Satoh, in: Thermal stress and strain in microelectronics packaging, ed. John H. Lau, New York: van Nostrand Reinhold (1993), p. 500.

16. W. J. Tomlinson and A. Fullylove, J. Mater. Sci. 27 5777 (1992).

17. J. C. Madeni, S. Liu, and T. A. Siewert, in: Proc. Int. Conf. Join. of Adv. and Specialty Materials, Milwaukee, WI (November 2001).

18. H. Mavoori and J. Chin, in: Proc. 45th ECTC, New York: IEEE (1995), p. 990.

19. J. S. Hwang and R. M. Vargas, Solder. Surf. Mount Technol. 5 38 (1990).

20. H. Mavoori, J. Chin, S. Vaynman, B. Moran, L. Keer, and M. Fine, J. Electron. Mater. 26 783 (1997).

21. C. J. Thwaites and W. B. Hampshire, Weld. J. Res. Suppl. 55 323s (1976).

22. L. Xiao, J. Liu, Z. Lai, L. Ye, and A. Tholen, in: Proc. Int. Symp. on Adv. Pack. Mater., Braselton, GA (March 6-8, 2000), p. 145.

23. D. A. Woodford, Trans. ASM 62 291 (1969).

24. F. A. Nichols, Acta Metall. 28 663 (1980).

25. J. H. Keeler, Trans. ASM 47 157 (1955).

26. Y. W. Cheng, R. L. Tobler, B. J. Filla, and K. J. Coakley, Constitutive behavior modeling of steels under hot-rolling conditions, National Institute of Standards and Technology, Boulder, CO, NIST Tech. Note 1500-6 (1999), 105 p.

Table 1. Young's modulus of 96.5Sn-3.5Ag solder

Young's modulus (E), GPa	Temperature (T), °C	References
$E = 2(1 + 0.35)[19.3 – 0.069(T)]$		3 (converted from shear modulus)
2.35	-50	10
2.35	20	
1.23	150	
57.12*	25	4
56.93*	25	
$E = 52.708 – 6.714 \times 10^{-2}(T) – 5.87 \times 10^{-5}(T)^2$		5, 8
56	25	6
26	25	7
2.4	20	15
$E^+ = 54.21 - 6.358 \times 10^{-2}(T) – 2.685 \times 10^{-5}(T)^2$		9
$E = 50.78 – 6.867 \times 10^{-2}(T) – 7.140 \times 10^{-5}(T)^2$		This study

* 96Sn-4Ag (This solder is included because Young's modulus is insignificantly affected by a small variation in composition.)
+ 95.5Sn-3.9Ag-0.6Cu (For the above same reason.)

Figure captions

Figure 1. Young's modulus of the 96.5Sn-3.5Ag solder as a function of temperature from different sources.

Figure 2. Engineering stress-strain curve for the 96.5Sn-3.5Ag solder (reproduced from reference 17). The specimen was tested at room temperature and at a strain rate of 2×10^{-4} s^{-1}.

Figure 3. Re-plot of figure 2 using true stress versus true plastic strain.

Figure 4. Comparison between prediction (solid line) and experimental data[17] (symbols). Specimens were tested at 25 °C and a strain rate of 2.0×10^{-4} s^{-1}.

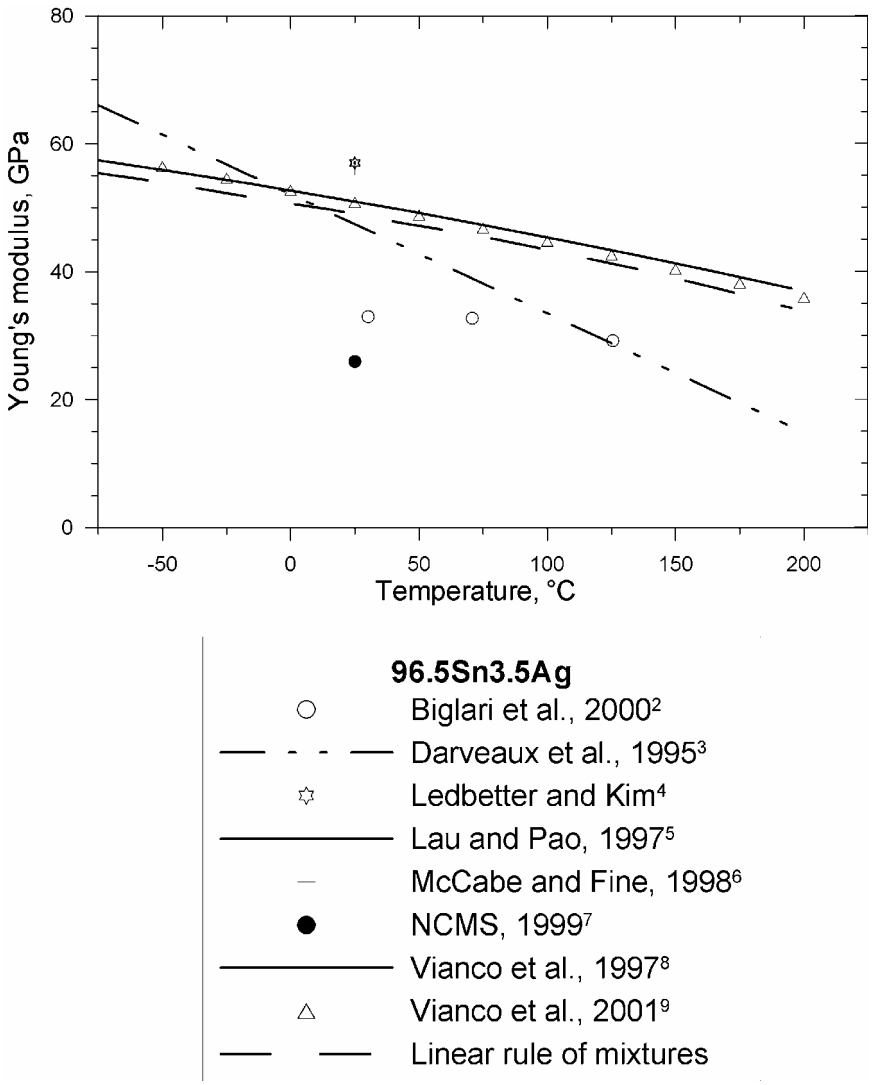

Figure 1. Young's modulus of the 96.5Sn-3.5Ag solder as a function of temperature from different sources.

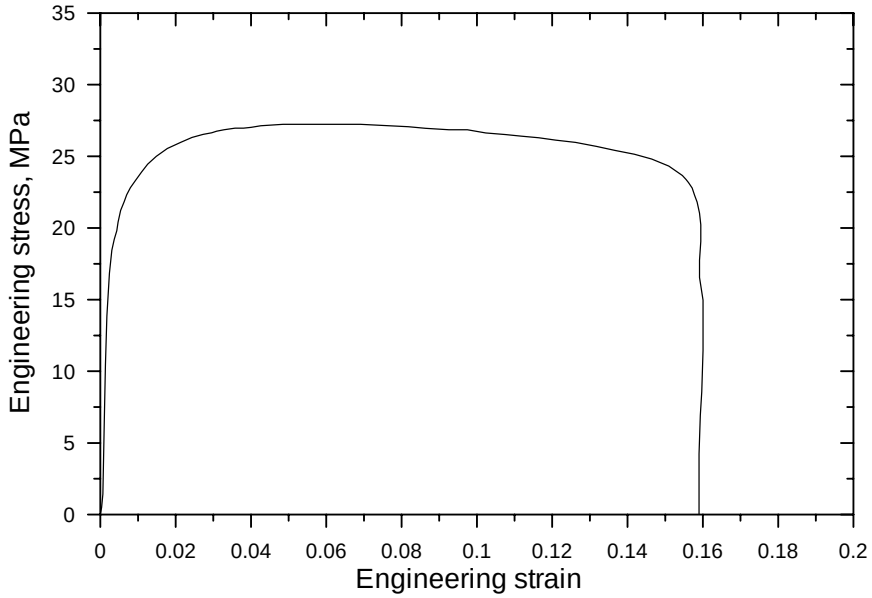

Figure 2. Engineering stress-strain curve for the 96.5Sn-3.5Ag solder (reproduced from reference 17). The specimen was tested at room temperature and at a strain rate of 2×10^{-4} s^{-1}.

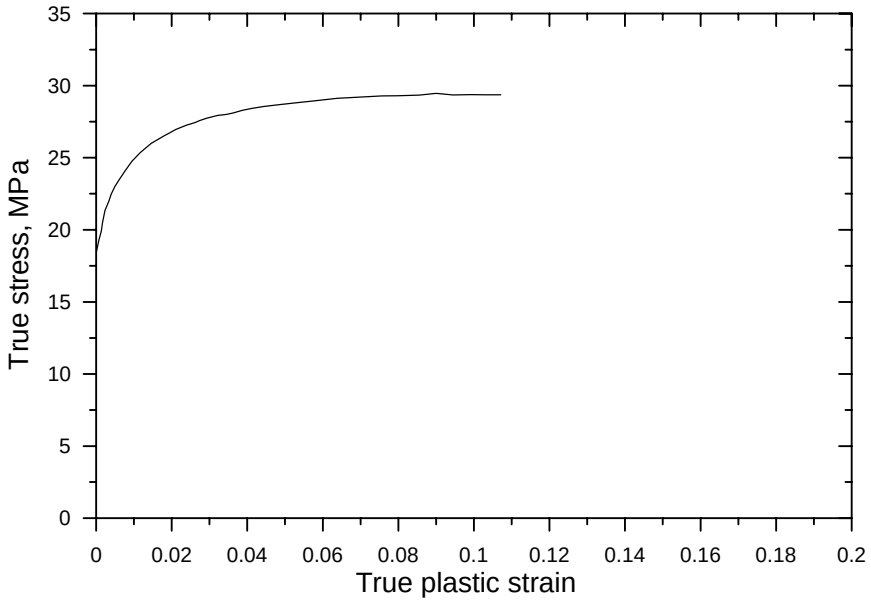

Figure 3. Re-plot of figure 2 using true stress versus true plastic strain.

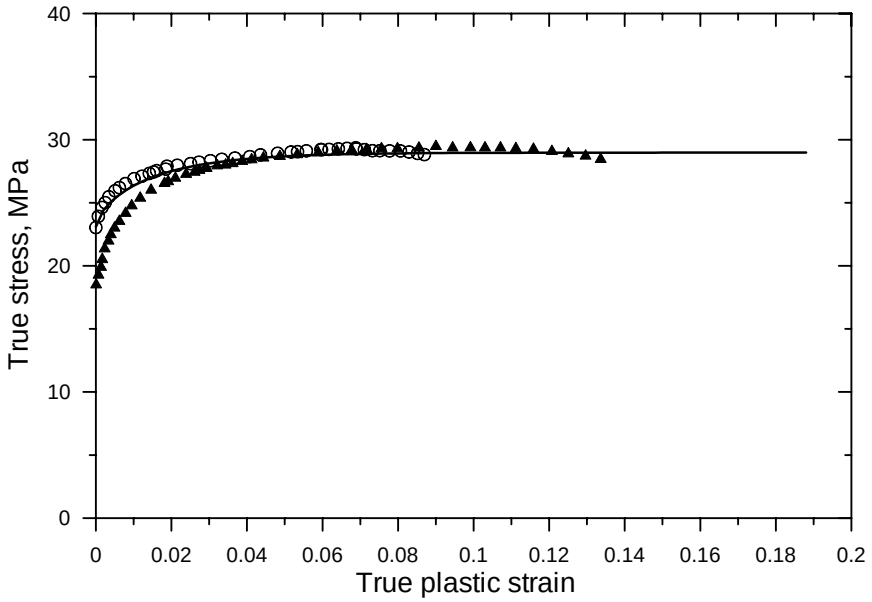

Figure 4. Comparison between prediction (solid line) and experimental data[17] (symbols). Specimens were tested at 25 °C and a strain rate of 2.0×10^{-4} s^{-1}.